ARTICLE

Large-Scale Patterning of Zwitterionic Molecules on a Si(111)-7 × 7 Surface

Mohamed El Garah,[†] Younes Makoudi,[†] Éric Duverger,[†] Frank Palmino,[†] Alain Rochefort,[‡] and Frédéric Chérioux[†,*]

[†]Institut FEMTO-ST, Université de Franche-Comté, CNRS, ENSMM, 32, Avenue de l'Observatoire, F-25044 Besançon Cedex, France, and [‡]Département de génie physique and Regroupement québécois sur les matériaux de pointe (RQMP), École Polytechnique de Montréal, CP 6079, Montréal, Canada H3C 3A7

ABSTRACT The formation of a large scale pattern on Si(111)-7 × 7 reconstruction is still a challenge. We report herein a new solution to achieve this type of nanostructuration by using of zwitterionic molecules. The formation of a large-scale pattern is successfully obtained due to the perfect match between the molecular geometry and the surface topology and to electrostatic interactions between molecules and surface. The adsorption is described by high-resolution scanning tunneling microscopy (STM) images and supported by density functional theory and STM calculations.

KEYWORDS: scanning tunneling microscopy · zwitterion · semiconductors · density functional theory calculations · self-assembly

*Address correspondence to frederic.cherioux@femto-st.fr.

Received for review September 10, 2010 and accepted November 15, 2010.

Published online November 24, 2010.
10.1021/nn102398g

For forty years, the top-down approach has led to an impressive amount of industrial and scientific results in the field of all-silicon microelectronics. Since the 1980's, π-conjugated molecules with large electronic conjugation paths and many remarkable designs have been developed by chemists to tune their electronic properties.[1,2] According to Moore's law, the scale of the next generation of semiconductor devices will be reduced to the nanometer range.[3−6] To reach these objectives, many techniques have been recently elaborated to converge both top-down and bottom-up approaches into the facile creation of low-dimensional systems on semiconducting surfaces that are based on π-conjugated molecules. Nowadays, the position and the dimension of the assemblies can be tuned and controlled with high precision, *i.e.*, down to the atomic level on metals[7−10] or semiconductors.[11−16] There are still several challenges in controlling the electronic properties of adsorbed assemblies since they can be deeply modified by strong molecules/semiconductor interactions. Developing new families of adsorbed assembly for semiconductor surfaces can overcome this problem, because the electronic skeleton of molecules is slightly altered after the adsorption.[17,18] Despite many attempts, the formation of a nearly complete molecular layer on a semiconductor surface without creating covalent bonds between molecules and substrate is rare, except for the few cases of halogen derivative adsorption on Si-based surfaces[19] or when boron atoms are inserted in the Si(111) surface.[20] In this paper, we propose a new, selective, and noninvasive way to achieve the first large-scale adsorbed molecular pattern at room temperature on Si(111)-7 × 7. The nature of the interactions has been elucidated by density functional theory (DFT) and by scanning tunneling microscopy (STM) calculations.

RESULTS AND DISCUSSION

STM experiments were performed with a VT-STM Omicron microscope installed in an ultrahigh-vacuum chamber with a base pressure lower than 2×10^{-10} mbar. STM images were acquired in constant-current mode at room temperature (RT). The 4-methoxy-*N*-(3-sulfonatopropyl)pyridinium (MSP) molecule was synthesized as a model of zwitterion, with a sulfonato group (SO_3^-) as the anionic site. The length of the molecule is 1.1 nm (Figure 1).

Deposition of the MSP molecules from a Mo crucible onto the sample at RT was performed at 333 K with a base pressure lower than 10^{-10} mbar. Then, high-resolution STM images of MSP/Si(111)-7 × 7 interface recorded at RT for two submonolayer coverages are shown in Figure 2.

In both cases, all protrusions are located on the faulted half-cells. For 0.1 monolayer (ML) coverage (Figure 2a), 49% of protru-

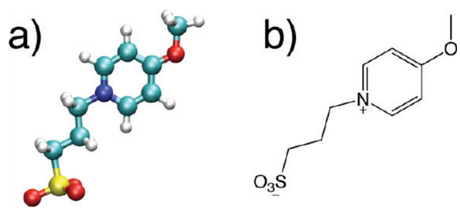

Figure 1. (a) Corey−Pauling−Koltun (CPK) model of the more stable conformation of isolated MSP optimized at DFT-local density approximation (DFT-LDA) level and (b) chemical structure of the MSP molecule.

sions is isolated (white arrow), 16.5% is coupled (white circle), and 34.5% has a triangular shape. For 0.21 ML coverage (Figure 2b), the number of isolated and paired protrusions decreases to 23.1 and 10.3%, respectively, whereas the number of triangles strongly increases to 66.6%.

The periodicity pattern (Figure 3a) is highlighted by the profile recorded along the black line in Figure 3b and corresponds to the surface periodicity. The diameter of each protrusion is nearly 0.8 nm, and its apparent height is around 1.1 nm.

Triangular nanostructures start to desorb from the surface at around 375 K, as proved by the STM image recorded (Figure 4).

High-resolution STM images of the same area obtained in the two polarities and at different bias voltages are described in Figure 5. In the empty states and for a bias voltage of Vs = +1.9 V (Figure 5a), the observed protrusions are located exactly over the three silicon rest-atoms marked as black points onto faulted half-cells. For a lower bias voltage [Vs = +0.9 V (Figure 5b)], the protrusions disappear, and a perfect Si(111)-7 × 7 is visible. In the filled states, the 7 × 7 reconstruction is observed again, but the six adatoms of faulted half-cells, containing protrusions in the empty states, are brighter than those of uncovered half-cells (black arrow, Figure 5c). We can also clearly see the presence of darker regions located in the vicinity of unfaulted (uncovered) half-cells that are due to a depletion of electron charge density.

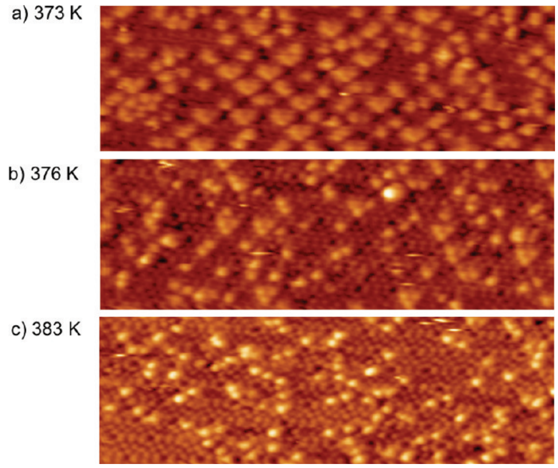

Figure 4. High-resolution STM images of the same area (40 × 17 nm^2, Vs = +1.6 V, It = 0.013 nA) of MSP deposited onto faulted half-cells of Si(111)-7 × 7 at: (a) 373, (b) 376, and (c) 383 K.

On the basis of experimental data, an empirical model for MSP adsorption on Si(111)-7 × 7 can be proposed. As shown in Figures 2, 3, and 5a, the diameter of each protrusion, always located over rest-atoms, is close to 0.8 nm, whereas the length of a MSP molecule is 1.1 nm. Therefore, one protrusion is attributed to one adsorbed MSP molecule normal to the substrate over the rest-atoms. Due to its lateral dimension (distance O−O ∼ 0.2 nm), a sulfonato group fits well between Si adatoms (distance Si−Si = 0.78 nm). Gas-phase zwitterions are more usually considered neutral,[21−23] which suggests an absence of negative charge accumulation on the sulfonato group (SO_3^-). Due to this electron lack, SO_3^- should be more eas-

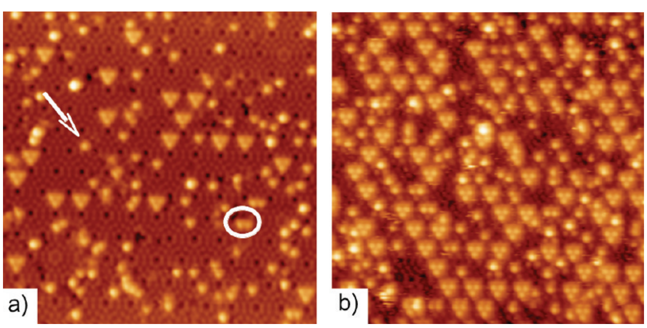

Figure 2. RT STM images showing triangular nanostructures constituted by MSP on a Si(111)-7 × 7 surface by increasing the molecule coverage from: (a) 0.1 ML to (b) 0.21 ML. Images were recorded in the same conditions (Vs = +1.7 V, It = 0.013 nA, 40 × 40 nm^2).

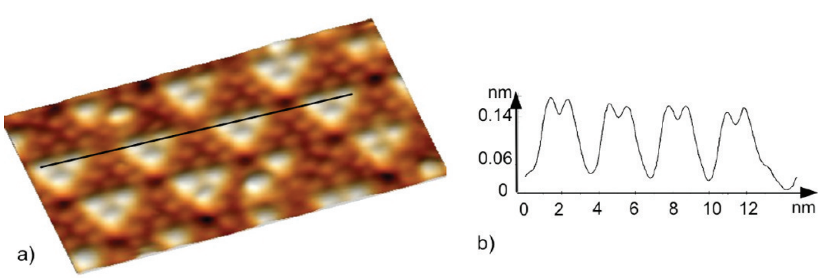

Figure 3. (a) STM image of MSP adsorbed onto faulted half-cells of Si(111)-7 × 7 (Vs = +1.9 V, It = 0.013 nA, 15 × 8 nm^2). (b) Apparent height in the profile recorded along the straight black line shown in (a).

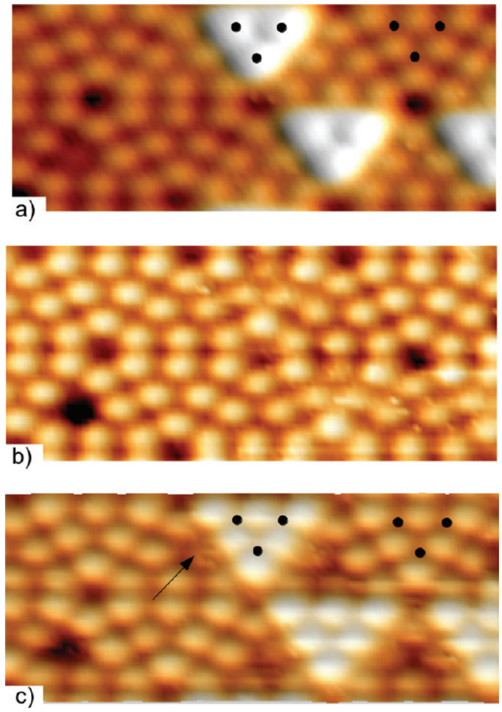

Figure 5. High-resolution STM images of the same area (10 × 5 nm^2) of MSP deposited onto faulted half-cells of Si(111)-7 × 7: (a and b) in the empty states, respectively, at Vs = +1.9 V, It = 0.013 nA and Vs = +0.9 V, It = 0.013 nA and (c) in filled states at Vs = −1.0 V, It = 0.013 nA. The black points correspond to the rest-atoms of the 7 × 7 reconstruction.

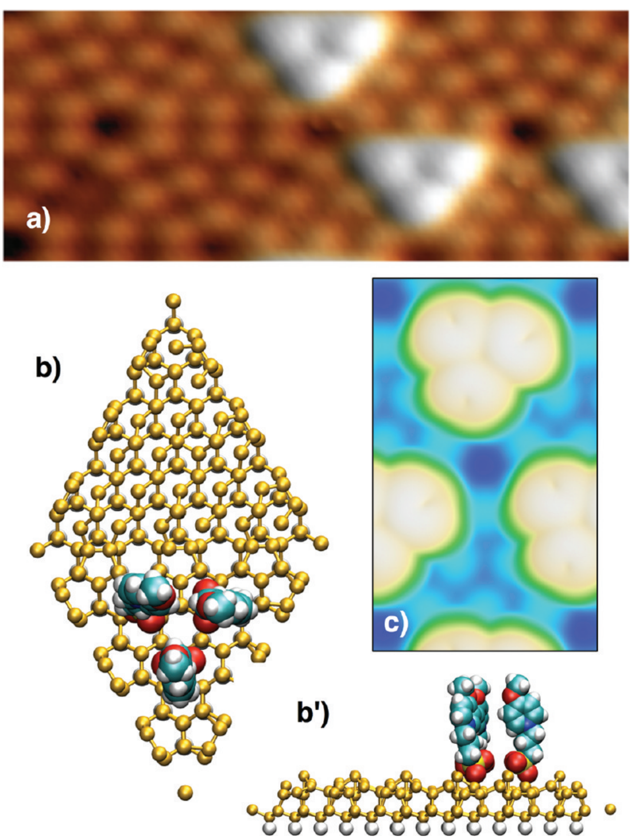

Figure 6. (a) High-resolution STM images of MSP molecules deposited on Si(111)-7 × 7 (Vs = +1.9 V, It = 0.013 nA, 8 × 5 nm^2). Optimized model of MSP triad adsorbed on a faulted half-cell of a Si(111)-7 × 7: (b) top and (b′) side views. (c) High-resolution simulated image (Pt(111) tip, Vs = +1.9 V, It = 0.01 nA) corresponding to a faulted half-cell of the supercell shown in (b).

ily attracted by electron-rich Si atoms located in faulted regions. Finally, to support an upright geometry for adsorbed MSP and a relatively high-desorption temperature, we can assume that the three O atoms of SO_3^- are significantly interacting with the adjacent surface Si adatoms.

In previous work, we demonstrated that zwitterions are adsorbed on a Si(111)-7 × 7 surface at RT. However, the nanostructures covered lower than 10% because the molecular design did not match the surface topology well enough.[24,25] In the present case, a coverage close to 21% is obtained with remarkable organic pattern of adsorbed MSP. The higher coverage is justified through the proposed empirical model, which shows a perfect match between the molecular geometry and the surface topology.

In order to support this empirical model, the adsorption of MSP on a Si(111)-7 × 7 surface was investigated with DFT calculations using the Vienna Ab-Initio Simulation Package (VASP).[26−28] The calculated adsorption energy is 0.37 eV by molecule in the supercell model shown in Figure 6b and b′), while it is 1.04 eV when a single MSP molecule is adsorbed. The calculated equilibrium bond distances are 0.27 and 0.30 nm for sulfur−silicon rest-atom and oxygen−silicon adatom, respectively (see Figure 6b′). Such large distances are incompatible with the presence of covalent bonds[15,16] and suggest that the MSP-substrate interaction is driven by electrostatic forces. Moreover, DFT calculations show that the presence of a triangle nanostructure in the faulted half-cell is favored over the unfaulted one by 0.35 eV. This result is in accordance with the well-known preferences of many adsorbates for the faulted half-cells.[29]

From the molecular coverage statistics up to 0.21 ML, we observe a decrease in the number of single structures and an increase of triangular ones, while the amount of paired protrusions remains nearly constant and low. Since MSP is deposited at 333 K, the preferential formation of triangle nanostructures can be described by the following scenario: (i) A single MSP is randomly adsorbed and then diffuses on more stable sites centered on faulted half-cells; (ii) the adsorption of MSP reduces the charge density of Si atoms near the adsorption site and in the unfaulted half-cell (see Figure 5); (iii) such decreasing electron density strongly hinders the adsorption of MSP in the unfaulted region and favors single molecule adsorption in the faulted half-cells; and (iv) due to an increasing amount of electron poor regions, the attractive intermolecular forces between MSP become more important than the MSP surface attractions, and this provokes a preferential formation of energetically more favorable triangle nanostructures.

STM simulations (see Figure 6c) on the optimized DFT adsorbed MSP/Si(111)-7 × 7 model were performed with the strongly parallel adaptive grid solvers scanning tunneling microscope (SPAGS-STM) software.[30] The simulated current constant image (Figure 6c) with this electron-scattering method reproduces the main experimental STM features, such as the three protrusions associated to the MSP triad as well as the surface structure of Si(111)-7 × 7 (see Figure 6a).

CONCLUSIONS

To sum up, a large molecular organic paving has been achieved at RT by two-dimensional template effects of the highly reactive Si(111)-7 × 7. We have highlighted that the adsorption without covalent bonds on silicon substrates can be achieved through electrostatic interactions by adequately designed molecules.

METHODS

Synthetic Method. MSP molecules have been synthesized by condensation of 4-methoxypyridine and 1,3-propane sultone (See Figure 7).

4-methoxypyridine was treated at 0 °C with 1 equiv of 1,3-propanesultone, leading to crystalline MSP. The white solid was purified by column chromatography (silica gel, acetone, R_f close to 0.5). The pure MSP was isolated as a white powder after evaporation of the solvent. RMN spectra were recorded on a AC-300 Bruker spectrometer: ^{1}H NMR (300 MHz, DMSO-D_6, 25 °C): $\delta = 2.14$ (quint., $^3J = 7.3$ Hz, 2H), 2.36 (t, $^3J = 7.3$ Hz, 2H), 4.07 (s, 3H), 4.54 (t, $^3J = 7.3$ Hz, 2H), 7.61 (d, $^3J = 8.7$ Hz, 2H), 8.86 (d, $^3J = 6.7$ Hz, 2H). ^{13}C NMR (80 MHz, DMSO-D_6, 25 °C): $\delta = 27.5$; 47.3; 57.9; 58.4; 113.7; 146.5; 170.8.

STM Experiments. The Si(111) substrate was heated under ultrahigh vacuum by direct current. Clean Si(111)-7 × 7 surface reconstruction was obtained by repeated cycles of heating at 1200 °C and slow cooling to RT. Deposition of the MSP molecules from an Mo crucible onto the sample at RT was performed at 60 °C and a base pressure lower than 10^{-10} mbar. STM experiments were performed with a VT-STM Omicron microscope installed in an ultrahigh vacuum chamber with a base pressure lower than 2×10^{-10} mbar. STM images were acquired in constant-current mode at RT.

Simulations. ***Electronic Structure Calculations.*** DFT calculations were carried out using the Vienna Ab Initio Simulation Package (VASP).[26−28]

The structure (slab) contained 333 atoms (200, Si; 3, N; 27, C; 3, S; 12, O; 88, H) separated by a vacuum spacer (15 Å) to form a periodic computation cell with a 7 × 7 unit cell of 249 atoms (200 Si atoms and 49 back-face H atoms). The accepted model for this surface is the dimer adatom stacking (DAS) fault model proposed by Takayanagi *et al.*[31] It contains 102 Si atoms related at the surface and one bilayer of the bulk Si(111)-1 × 1 (98 Si atoms). H atoms were used to saturate the silicon dangling bonds at the bottom of the slab structure.

The atomic positions of the MSP molecules as well as the whole Si(111)-7 × 7 slab were fully optimized using the force and the total-energy minimum RMM-DIIS minimization algorithm until a numerical accuracy better than 5×10^{-2} eV/Å for the total forces and an energy variation lower than 10^{-4} eV were reached.[32] The generalized gradient corrected approximation functional Perdew−Burke−Ernzerhof and a plane wave cutoff of 400 eV were used.[33] The Monkhorst−Pack *k*-point grid was used corresponding to the γ point in the unit cell.[34]

STM Simulations. STM simulations were performed with the strongly parallel adaptive grid solvers STM (SPAGS-STM) software to evaluate topographic mode images and scanning tunneling spectra (STS). The software includes several algorithmic strategies such as parallel computation of the tunnel currents[30] and adaptive grids that minimize the probing sites needed to obtain a high-resolution image.[35,36] In STM simulations, the tunnel current was computed within a scattering approach based on the Landauer−Büttiker formalism[37] along with an extended Hückel theory Hamiltonian.[38]

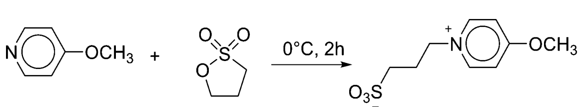

Figure 7. Synthesis of MSP.

Acknowledgment. This work was supported by the Communauté d'Agglomération du Pays de Montbéliard, the région de Franche-Comte, and the French Agency ANR (ANR-07-JCJC-0053). Computational support was provided by IDRIS (Orsay, France) and Réseau québécois de calcul de haute performance (RQCHP).

REFERENCES AND NOTES

1. MacDiarmid, A. G. Synthetic metals: A Novel Role for Organic Polymers (Nobel lecture). *Angew. Chem., Int. Ed.* **2001**, *40*, 2581–2590.
2. Heeger, A. J. Semiconducting and Metallic Polymers: The Fourth Generation of Polymeric Materials (Nobel lecture). *Angew. Chem., Int. Ed.* **2001**, *40*, 2591–2611.
3. Joachim, C.; Gimzewski, J. K.; Aviram, A. Electronics Using Hybrid-Molecular and Mono-Molecular Devices. *Nature* **2000**, *408*, 541–548.
4. Ratner, M. Molecular Electronics - Charged With Manipulation. *Nature* **2005**, *435*, 575–577.
5. Rochefort, A.; Martel, R.; Avouris, Ph. Electrical Switching in Pi-Resonant 1D Intermolecular Channels. *Nano Lett.* **2002**, *2*, 877–880.
6. Piva, P. G.; DiLabio, G. A.; Pitters, J. L.; Zikovski, J.; Rezeq, M.; Dogel, S.; Hofer, W. A.; Wolkow, R. A. Field Regulation of Single-Molecule Conductivity by a Charged Surface Atom. *Nature* **2005**, *435*, 658–661.
7. Barth, J. V.; Constantini, G.; Kern, K. Engineering Atomic and Molecular Nanostructures at Surfaces. *Nature* **2005**, *437*, 671–679.
8. Theobald, J. A.; Oxtoby, N. S.; Philipps, N. A.; Champness, N. R.; Beton, P. H. Controlling Molecular Deposition and Layer Structure with Supramolecular Surface Assemblies. *Nature* **2003**, *424*, 1029–1031.
9. Percec, V.; Glodde, M.; Bera, T. K.; Miura, Y.; Shiyanovskaya, I.; Singer, K. D.; Balagurusamy, V. S. K.; Heiney, P. A.; Schnell, I.; Rapp, A. Self-Organization of Supramolecular Helical Dendrimers into Complex Electronic Materials. *Nature* **2002**, *419*, 384–387.
10. Grill, L.; Dyer, M.; Lafferentz, L.; Perssson, M.; Peters, M. V.; Hecht, S. Nano-Architectures by Covalent Assembly of Molecular Building Blocks. *Nat. Nanotechnol.* **2007**, *2*, 687–691.
11. Lu, P. H.; Polanyi, J. C.; Rogers, D. Photoinduced Localized Atomic Reaction (LAR) of 1,2- and 1,4-Dichlorobenzene with Si(111)-7 × 7. *J. Chem. Phys.* **2000**, *112*, 11005–11010.
12. McNab, I. R.; Polanyi, J. C. Patterned Atomic Reaction at Surfaces. *Chem. Rev.* **2006**, *106*, 4321–4354.
13. Hossain, M. Z.; Kato, H. S.; Kawai, M. Self-Directed Chain Reaction by Small Ketones with the Dangling Bond Site on the Si(100)-2 × 1-H Surface: Acetophenone, a Unique Example. *J. Am. Chem. Soc.* **2008**, *130*, 11518–11523.
14. Lopinski, G. P.; Wayner, D. D. M.; Wolkow, R. A. Self-Directed Growth of Molecular Nanostructures on Silicon. *Nature* **2000**, *406*, 48–51.
15. Hamers, R. J.; Coulter, S. K.; Ellison, M. D.; Hovis, J. S.; Padowitz, D. F.; Schartz, M. P.; Greenlief, C. M.; Russel, J. N. Cycloaddition Chemistry of Organic Molecules with Semiconductor Surfaces. *Acc. Chem. Res.* **2000**, *33*, 617–624.
16. Hurley, P. T.; Nemanick, E. J.; Brunschwig, B. S.; Lewis, N. S. Covalent Attachement of Acetylene and Methylacetylene Functionality to Si(111) Surfaces: Scaffolds for Organic

Surface Functionalization While Retaining Si-C Passivation of Si(111) Surface Sites. *J. Am. Chem. Soc.* **2006**, *128*, 9990–9991.
17. Harikumar, K. R.; Polanyi, J. C.; Sloan, P. A.; Ayissi, S.; Hofer, W. A. Electronic Switching of Single Silicon Atoms by Molecular Field Effects. *J. Am. Chem. Soc.* **2006**, *128*, 16791–16797.
18. Harikumar, K. R.; Lim, T. B.; McNab, I. R.; Polanyi, J. C.; Zotti, L.; Ayissi, S.; Hofer, W. A. Dipole-Directed Assembly of Lines of 1,5-Dichloropentane on Silicon Substrates by Displacement of Surface Charge. *Nat. Nanotechnol.* **2008**, *3*, 222–228.
19. Lu, X. K.; Polanyi, J. C.; Yang, J. A Reversible Molecular Switch Based on Pattern-Change in Chlorobenzene and Toluene on a Si(111)-7 × 7 Surface. *Nano Lett.* **2006**, *6*, 809–814.
20. Makoudi, Y.; Arab, M.; Palmino, F.; Duverger, E.; Cherioux, F. Complete Supramolecular Self-Assembled Adlayer on a Silicon Surface at Room Temperature. *J. Am. Chem. Soc.* **2008**, *130*, 6670–6671.
21. Price, W. D.; Jockusch, R. A.; Williams, E. R. Is Arginine a Zwitterion in the Gas Phase. *J. Am. Chem. Soc.* **1997**, *119*, 11988–11989.
22. Chapo, C. J.; Paul, J. B.; Provencal, R. A.; Roth, K.; Saykally, R. J. Is Arginine Zwitterionic or Neutral in the Gas Phase? Results from IR Cavity Ringdown Spectroscopy. *J. Am. Chem. Soc.* **1998**, *120*, 12956–12957.
23. Nazmutdinov, R. R.; Zhang, J.; Zinkicheva, T. T.; Manyurov, I. R.; Ulstrup, J. Adsorption and *in situ* Scanning Tunneling Microscopy of Cysteine on Au(111): Structure, Energy, and Tunneling Contrasts. *Langmuir* **2006**, *22*, 7556–7567.
24. Makoudi, Y.; Arab, M.; Palmino, F.; Duverger, E.; Picaud, F.; Ramseyer, Ch.; Cherioux, F. A Stable Room-Temperature Molecular Assembly of Zwitterionic Organic Dipoles Guided by a Si(111)-7 × 7 Template Effect. *Angew. Chem., Int. Ed.* **2007**, *46*, 9287–9290.
25. Makoudi, Y.; El Garah, M.; Palmino, F.; Duverger, E.; Arab, M.; Cherioux, F. Adsorption of an Organic Zwiterrion on a Si(111)-7 × 7 Surface at Room Temperature. *Surf. Sci.* **2008**, *602*, 2719–2723.
26. Kresse, G.; Furthmuller, J. Efficient Iterative Schemes for *ab initio* Total-Energy Calculations Using a Plane-Waves Basis Set. *Phys. Rev. B: Condens. Matter Mater. Phys.* **1996**, *54*, 11169–11186.
27. Blochl, P. E. Projected Augmented-Wave Method. *Phys. Rev. B: Condens. Matter Mater. Phys.* **1994**, *50*, 17953–17979.
28. Kresse, G.; Hafner, J. Ab initio Molecular-Dynamics for Open-Shell Transition-Metals. *Phys. Rev. B: Condens. Matter Mater. Phys.* **1993**, *47*, 558–561.
29. Vasco, E. Mechanisms of Preferential Adsorption on the Si(111)-7 × 7 Surface. *Surf. Sci.* **2005**, *575*, 247–249.
30. Janta-Polczynski, B.; Cerdá, J. I.; Éthier-Majcher, G.; Piyakis, K.; Rochefort, A. Parallel Scanning Tunneling Microscopy Imaging of Low Dimensional Nanostructures. *J. Appl. Phys.* **2008**, *104*, 023702.
31. Takayanagi, K.; Tanishiro, Y.; Takahashi, S.; Takahashi, M. Structural Analysis of Si(111)-7 × 7 Reconstructed Surface by Transmission Electron Diffraction. *Surf. Sci.* **1985**, *164*, 367–392.
32. Perdew, J. P.; Burke, K.; Ernzerhof, M. Generalized Gradient Approximation Made Simple. *Phys. Rev. Lett.* **1996**, *77*, 3865–3368.
33. Monkhorst, H. J.; Pack, J.-D. Special Points for Brillouin-Zone Integrations. *Phys. Rev. B: Solid State* **1976**, *13*, 5188–5192.
34. Csaszar, P.; Pulay, P. Predicted Vibrational Frequencies and Assignment of the Spectra of Uracil and its N, N-Dideutero Derivative by Quantum Chemical Methods. *J. Mol. Struct.* **1984**, *114*, 31–34.
35. Eckert, F.; Pulay, P.; Werner, H.-J. Ab initio Geometry Optimization for Large Molecules. *J. Comput. Chem.* **1997**, *18*, 1473–1483.
36. Bedwani, S.; Guibault, F.; Rochefort, A. Nanoscale Adaptive Meshing for Rapid STM Imaging. *J. Comput. Phys.* **2008**, *227*, 6720–6726.
37. Büttiker, M.; Imry, Y.; Landauer, R.; Pinhas, S. Generalized Many-Channel Conductance Formula with Application to Small Rings. *Phys. Rev. B: Condens. Matter Mater. Phys.* **1985**, *31*, 6207–6215.
38. Cerdá, J. I.; Van Hove, M. A.; Sautet, P.; Salmeron, M. Efficient Method for the Simulation of STM Images. I. Generalized Green-function formalism. *Phys. Rev. B: Condens. Matter Mater. Phys.* **1997**, *56*, 15885–15899.